IEEE Access
Multidisciplinary | Rapid Review | Open Access Journal

Received 5 January 2024, accepted 23 January 2024, date of publication 25 January 2024, date of current version 5 February 2024.

Digital Object Identifier 10.1109/ACCESS.2024.3358686

RESEARCH ARTICLE

Advancing Breast Cancer Detection: Enhancing YOLOv5 Network for Accurate Classification in Mammogram Images

MUHAMMAD ANAS[1], IHTISHAM UL HAQ[2], GHASSAN HUSNAIN[3], AND SYED ALI FARAZ JAFFERY[4]

[1]Department of Electrical Engineering, University of Gujrat, Hafiz Hayat Campus, Gujrat 50700, Pakistan
[2]Department of Mechatronics Engineering, University of Engineering and Technology Peshawar, Peshawar 25000, Pakistan
[3]Department of Computer Science, CECOS University of IT and Emerging Sciences, Peshawar 25100, Pakistan
[4]Department of Electrical Engineering, University of Engineering and Technology Taxila, Taxila 47050, Pakistan

Corresponding authors: Muhammad Anas (iamengranas@gmail.com) and Ihtisham Ul Haq (16pwmct0478@uetpeshawar.edu.pk)

ABSTRACT Recent advances in artificial intelligence (AI), notably deep learning, have sparked widespread curiosity with bioinformatics, particularly the challenges presented by medical imaging. It's been really helpful in enabling the Computer Aided Diagnosis CAD system to provide precise outcomes. Nonetheless, it is still a difficult task to identify breast cancer in mammography images. The purpose of this effort is to lower False Positive Rate FPR and False Negative Rate FNR and increase Matthews's correlation coefficient MCC value. Two highly tailored object detection models, YOLOv5 and Mask R-CNN, are utilized to get the job done. YOLOv5 is able to detect the mass and determine whether it is benign or malignant. However, YOLOV5's limited real estate necessitates certain tweaks to the original model in order to get the desired effects. Tumor borders and size are both identified by Mask RCNN as it traverses breast parenchyma in search of malignancies. Stages of cancer are based on the magnitude of the patients' tumours. This model employs YOLOv5+Mask RCNN and is trained on the INbreast, CBIS-DDSM, and BNS dataset. The proposed model is compared against the baseline version of YOLOv5 to determine how well it performs. The proposed method improves performance, with an FPR of 0.049%, a FNR of 0.029%, and a high MCC value of 92.02%. Based on the results of the studies, combining YOLOv5 with Mask RCNN improves accuracy by 0.06 percentage points compared to using either method alone. Furthermore, this effort may aid in determining the patient's prognosis and allowing clinicians to be more accurate and predictable in the diagnosing process at an early stage.

INDEX TERMS Breast cancer detection, deep learning, YOLOV5, mammogram images, mask RCNN.

I. INTRODUCTION

Breast cancer is the primary contributor to mortality from cancer in women on a global scale and represents one of the most prevalent forms of invasive malignancies affecting the female population. This condition has the potential to impact individuals of all genders across various age groups, with a higher prevalence observed among individuals in middle age and older. In the year 2018, it is anticipated that a total of 627,000 individuals experienced mortality, while an additional 2.1 million incidents were documented. While there are other types of cancers that are more prevalent in women, such as cervical, lung, and thyroid cancers, breast cancer remains a significant concern, representing around 25% of all cancer cases globally [1]. According to the World Health Organisation (WHO), it is projected that there will be around 19.3 million newly diagnosed cases of cancer by the year 2025 [2]. Numerous studies have demonstrated an upward trend in breast cancer mortality rates across various global regions and age cohorts. The global prevalence

The associate editor coordinating the review of this manuscript and approving it for publication was Larbi Boubchir.

of breast cancer is increasing among individuals of all age groups. However, it is particularly prominent among women who are under the age of 50 and have not yet reached menopause [3]. The incidence rates of breast cancer, adjusted for age, indicate that Pakistan exhibits one of the highest rates compared to other Asian countries [4]. According to a study, the incidence of breast cancer among Asian women is estimated to be approximately 1 in 9 [5]. The country experiences a notable and increasing prevalence of breast cancer. However, the death rate remains elevated due to factors such as delayed detection, regional and cultural limitations, insufficient diagnostic resources, and a scarcity of treatment centres. Based on the findings of several research conducted globally, it has been shown that timely identification and intervention in cases of breast cancer are pivotal factors in achieving favourable outcomes. The prognosis for a patient with cancer diagnosed at an early stage is significantly more favourable compared to a patient with cancer detected at a later, more advanced stage. To achieve a significant reduction in long-term morbidity and mortality rates, it is imperative to enhance public knowledge on the importance of regular screenings, timely diagnosis of symptoms, and appropriate treatment [6]. The inadequate dissemination of knowledge regarding breast cancer diagnosis and treatment among women in Pakistan, particularly those residing in rural regions, can be attributed to a multitude of causes [7]. As a consequence, a significant proportion of breast cancer patients, specifically 88.9%, are diagnosed in the later stages, while 58.8% are identified at an advanced stage, as reported in reference [8]. Breast cancer exhibits a significant and escalating fatality rate within the nation, primarily attributable to delayed diagnosis, regional and cultural obstacles, insufficient technological advancements in diagnostics, and inadequate availability of treatment resources. Numerous studies and research endeavours done globally have consistently arrived at a shared consensus: timely identification and intervention play a pivotal role in achieving successful remission of breast cancer. Individuals who receive a cancer diagnosis at an early, non-metastatic stage exhibit a higher likelihood of achieving complete remission and experiencing extended survival compared to those who are diagnosed at a later, metastatic stage. Raising public awareness regarding the significance of regular screening is of utmost importance. Early identification of symptoms and subsequent intervention are imperative in substantially reducing mortality and morbidity rates. Mammograms, however very efficacious in the early detection of breast cancer, are not exempt from inherent limitations. Mammography stands as the sole diagnostic imaging examination that has been substantiated to effectively diminish fatality rates associated with breast cancer. Asymptomatic women with an average risk profile often commence annual testing at approximately 40 years of age. Mammography employs low intensity x-rays to generate pictures, enabling the detection of ductal carcinoma in situ (DCIS) and calcification prior to their palpable manifestation. Breast cancer and its corresponding calcifications are visually detected on mammograms as luminous and asymmetrical areas. Mammography is widely recognised as the foremost tool for identifying breast cancer due to its effectiveness in early diagnosis and its potential to reduce breast cancer-related mortality. The radiological diagnosis may provide challenges due to the potential for misinterpretation of small calcifications and poor contrast imaging characteristics [7]. Hence, computer-aided diagnosis (CAD) provides an additional perspective to facilitate accurate diagnostic outcomes. This technology has the capability to detect changes that may not be perceptible to the unaided human eye. This study may additionally contribute to the identification of the kind of tumours, distinguishing between benign and malignant cases, and assisting in the diagnosis of breast pathologies. There are two primary forms of breast tumours, namely malignant and nonmalignant tumours [8]. Cysts and fibroadenomas represent two instances of benign neoplasms. The objects exhibit well-defined contours without any rough edges or blurring. The carcinoma in situ designation is used by medical professionals to describe tumours that have not metastasized to other body regions. Malignant and aggressive characteristics are commonly observed in milk duct malignancies. The aberrant spread of these cells initially occurs inside the breast parenchyma, followed by dissemination to other parts of the body [9]. The timely recognition and treatment of aberrant cell growth are essential for effectively managing its uncontrolled proliferation. Individuals who were diagnosed early and had timely treatment demonstrated a 100% survival rate, but those who experienced a delayed diagnosis and treatment exhibited a survival rate of 0%. This implies that the timely detection and identification of cancer by routine screening may prevent its metastasis to other bodily organs [10].

The utilisation of the Matthews Correlation Coefficient (MCC) as a comprehensive measure of a classifier's performance, as opposed to accuracy alone, is supported by research [11]. Numerous researchers have diligently endeavoured to develop networks that exhibit promising outcomes in the pursuit of a reliable modality for breast tumour diagnosis. The exploration of false positive and false negative rates, together with Matthew's correlation coefficient (MCC) values, remains mostly uncharted in the realm of academic research. In the context of binary classification, the Matthews Correlation Coefficient (MCC) is considered a more reliable metric compared to accuracy. However, it necessitates consistently high performance across all categories in the confusion matrix. In pursuit of this objective, our research makes significant contributions by: In this study, we provide a novel approach utilising mammograms to develop a model capable of effectively identifying and classifying breast tumours into two distinct categories: benign or malignant. The methodology employed in this study aims to reduce both the False Positive Rate (FPR) and False Negative Rate (FNR) while maintaining precision and accuracy. The Matthews Correlation Coefficient (MCC) is a significant performance statistic that is subject to continuous improvement efforts. To identify the most effective approach for detecting and classifying

breast tumours, we utilise all four variants (Small, medium, large and extra large) of the YOLOv5 model. Additionally, we conduct a comparative analysis between our proposed model and the most advanced networks currently available in order to offer a comprehensive evaluation of its performance. The objective is to develop a computational model capable of accurately identifying breast masses in mammograms and subsequently classifying them as either malignant or benign. The misclassified data is subjected to a secondary model in order to accurately determine the boundaries and size of tumours, which serve as important indications of the stage of cancer. By reducing the False Negative Rate (FNR) and False Positive Rate (FPR) while maintaining accuracy, the Matthews Correlation Coefficient (MCC) is enhanced. The assessment of the system's performance could be achieved by comparing the outcomes of the proposed model with those of established models. The paper is structured into five distinct sections. Section II presents a comprehensive review of the existing literature. Section III outlines our suggested technique. Section IV provides an in-depth analysis of the experiments conducted and presents the corresponding results. Finally, Section V concludes the paper and discusses potential avenues for future research.

II. LITERATURE REVIEW

The importance of precise and thorough picture analysis and interpretation cannot be overstated in the field of medical research. Radiologists and physicians possess enhanced capabilities in the detection and identification of abnormalities. In their study, researchers presented a framework for the categorization of breast masses using Computer-Aided diagnosis (CAD) techniques [13]. This study utilises data obtained from the Mammographic Image Analysis Society (MIAS), data collected by the researchers themselves, and data sourced from the Digital Database for Screening Mammography (DDSM). The system preprocesses, segments, collects, and groups functions. The Computer-Aided Diagnosis (CAD) programme employs a convolutional neural network (CNN) architecture consisting of eight coevolutionary layers, four max-pooling layers, and two fully connected layers. Subsequently, a comparative analysis is conducted between the accuracy and AUC (Area Under the Curve) of the proposed Convolutional Neural Network (CNN) and two other pretrained networks, namely Alex Net and VGG16. The results of this analysis demonstrate that the recommended CNN exhibits superior effectiveness in comparison. The proposed model demonstrated an accuracy of 92.54% on the MIAS dataset, 96.47% on the DDSM dataset, and 95% on the self-collected dataset. Additionally, the corresponding AUC scores for these datasets were 0.85, 0.96, and 0.94, respectively. In [14], the authors successfully employed an extreme learning technique to perform feature fusion mapping and extract CNN features for the purpose of breast cancer diagnosis and classification. The author proposes the utilisation of a multi-deep convolutional neural network (DCNN) framework as a means of categorising breast cancer. The objective of this project is to enhance the accuracy of breast cancer diagnosis through the utilisation of deep learning algorithms. The methodology utilises a combination of deep convolutional neural networks (DCNNs) to examine mammograms and ascertain their classification as either malignant or non-cancerous. The study presents the experimental findings and validation of the proposed framework, demonstrating its capability to reach a high level of classification accuracy. These results indicate significant potential for computational advancements in the field of breast cancer diagnostics. The present study [15] introduces a theoretical framework aimed at the automated identification, classification, and partitioning of breast cancer in mammographic images. This study employs the MIAS and CBIS-DDSM databases for analysis. This study employs a sample of pictures that is relatively restricted in size. Preprocessing often include the removal of muscle sections that may yield false-positive results, along with the reduction of artefacts and noise. The implementation of a median filter has the potential to mitigate noise present in mammograms. The images undergo a processing procedure wherein the tumour is rendered imperceptible through the isolation of the muscular structures, followed by the conversion of the images into distinct patches. The efficiency of the system is enhanced by converting the preprocessed image into patches of size 512-512. Subsequently, the MASK-RCNN and Deep Lab deep learning models are employed for the purpose of identifying the presence and location of malignancy. The results of this study indicate that MASK-RCNN achieved an Area Under the Curve (AUC) value of 0.98, whereas Deep Lab exhibited an AUC of 0.95. In the context of the segmentation task, the achieved mean average accuracy scores are 0.80 and 0.75. The precision of the radiologist ranged from 0.80 to 0.88. Hence, this research contributes to the assistance provided to radiologists in the categorization of breast tumours. Nonetheless, additional investigation is required to attain the most favourable outcomes. In the present investigation [16], the author puts forth the employment of a YOLO detector using DDSM and breast datasets for the purpose of detecting breast cancer tumours. The effectiveness of this approach is evident from the DDSM dataset, which achieved a score of 99.28%, and the INbreast dataset, which achieved a score of 98.02%. However, it is important to note that the high false positive rate (FPR) of 14% is a notable drawback. A novel approach to cancer classification was introduced, employing feedforward Convolutional Neural Networks (CNNs) such as ResNet-50 and Inception ResNet-V2. In the study conducted by [17], it was observed that all three approaches demonstrated an accuracy of 90% or above on both datasets. Specifically, the False Positive Rate (FPR) for the breast dataset increased to 28.57% for the CNN approach, 14.28% for the Res-Net50 approach, and 16.66% for the Inception ResNet V2 approach. This paper presents a proposed approach for the segmentation and classification of breast cancer tumours using an updated version of the Firefly algorithm combined with the chicken swarm optimisation (FC-CSO) and the region-based convolutional

neural network (RCNN). The proposed approach is applied to the MIAS dataset. The aforementioned methodology exhibits a notable level of precision (93%), responsiveness (97%), selectivity (92%), False Positive Ratio (FPR) (7%), and false negative ratio (FNR) (3%), while demonstrating a relatively diminished level of certainty (MCC) (85%). In their study, the authors of reference [18] propose a methodology that utilizes the Convolutional Neural Network (CNN) model and the Mammographic Image Analysis Society (MIAS) dataset. This approach aims to extract distinctive features and perform classification of breast cancer tumours. The method yielded favourable outcomes, including a 95-percent accuracy, 98-percent sensitivity, 90-percent specificity, and a 2-percent false-negative rate. However, it is important to note that the Matthews correlation coefficient (MCC) value reduces to 89% and the false positive rate (FPR) decreases to 10%. By employing neural networks, the approach proposed in the study demonstrated a high level of accuracy in predicting the five-year survival of breast cancer patients. The researchers employed the Wisconsin Breast Cancer Dataset for both the training and evaluation phases of an artificial neural network (ANN) [19]. The study demonstrated state-of-the-art performance by utilizing the Just Neural Network (JNN) framework and conducting experiments on the Haberman's Breast Cancer Survival dataset obtained from UC Berkeley's Centre for Machine Learning and Intelligent Systems. The ultimate level of precision achieved was 88.24%. The study titled "Delay-Multiply-and-Sum (DMAS): A Proposed Method for Achieving Ultra-Wideband Confocal Microwave Imaging" introduced a technique for achieving ultra-wideband confocal microwave imaging. In comparison to the DAS imaging method, this technique produced outcomes of higher precision. The technique of conformal predictors was founded upon the utilisation of rule-based genetic algorithms [20]. The efficacy of the technique was tested using two datasets, one comprising breast cancer cases and the other involving ovarian cancer cases. The technique successfully presented the prediction zones. The superior performance of this technique can be attributed to its comprehensible rules, which surpassed those of other conformal predictors. The study demonstrated that ResNet and Inception achieved superior performance compared to the YOLO series, with accuracy levels of 91% and 95.5% respectively (Reference). Recent research investigations employing diverse conventional methods for cancer diagnosis have demonstrated remarkably high levels of accuracy, reaching up to 99%. Insufficient emphasis has been given to the misclassification ratio and the Matthews correlation coefficient (MCC) score. When dealing with binary classifications, it is a valid method to calculate accuracy using confusion matrices, especially when the data sets are evenly distributed. Nevertheless, the Matthews Correlation Coefficient (MCC) emerges as a more reliable statistical measure in cases where the dataset exhibits an imbalance. The numerical value in question has a large magnitude alone in cases where each of the four divisions within the confusion matrix precisely forecasts positive results. Moreover, the Matthews Correlation Coefficient (MCC) exhibits a high value when both the False Negative Rate (FNR) and False Positive Rate (FPR) are minimized. The utilisation of high accuracy as the sole criteria for assessing positive prognosis in clinical diagnosis may lead to severe repercussions [21]. The author describes CAD for breast cancer [22]. This project aims to improve breast cancer diagnosis by establishing a robust classification system with numerous classifiers. The CAD system analyses mammograms to determine lesion malignancy using machine learning techniques. The study provides empirical evidence that the suggested Computer-Aided Diagnosis (CAD) system can detect and diagnose breast cancer with high accuracy and sensitivity. The study suggests that computer-assisted breast cancer diagnosis could be improved. The author in [23] highlights the utmost significance of security in the digital age, specifically when it comes to transmitting images over networks. It emphasizes the importance of achieving authenticity and confidentiality through a robust two-level security mechanism. This involves concealing images using stenographic methods to ensure authenticity and encrypting them with 2D Cellular Automata rules to maintain confidentiality. This two-tiered approach guarantees heightened security, with each level bolstering the other in the event of a breach. Academics [24] studied how deep learning could improve mammography cancer diagnosis. This study examines if sophisticated deep learning algorithms can improve breast cancer detection by studying mammograms. The study describes the picture preparation and deep learning models used. The study found that deep learning improves cancer diagnosis mammography accuracy and patient outcomes. This research advances breast cancer computer-aided diagnosis approaches, which may improve early detection and patient outcomes. Researchers describe a unique histopathology image analysis method for breast cancer diagnosis. Histo-CADx uses two-stage fusion to improve breast cancer detection. Deep learning is used to extract useful properties from histopathology pictures. To incorporate these collected characteristics, cascaded fusion is used. This document covers Histo-CADx's preprocessing, feature extraction, and fusion methods. The experimental results show that the proposed framework can accurately diagnose breast cancer using histological pictures. This study expands knowledge on computer-aided detection tools for breast cancer, highlighting their potential to enhance accuracy and simplify treatment decisions. If the algorithm predicted a false positive tumour, the patient would likely incur physical pain through biopsy or surgery and psychological trauma. If the model mispredicts the lack of malignancies, the condition could be fatal. Thus, a reliable model that decreases the false positive rate (FPR), false negative rate (FNR), and Matthews correlation coefficient (MCC) score is crucial [26]. Significant progress is made in by the introduction of a multimodal system that integrates numerous data sources for sleep staging. The novel approach of using salient wave recognition to conduct sleep stage analysis is a significant step forward.

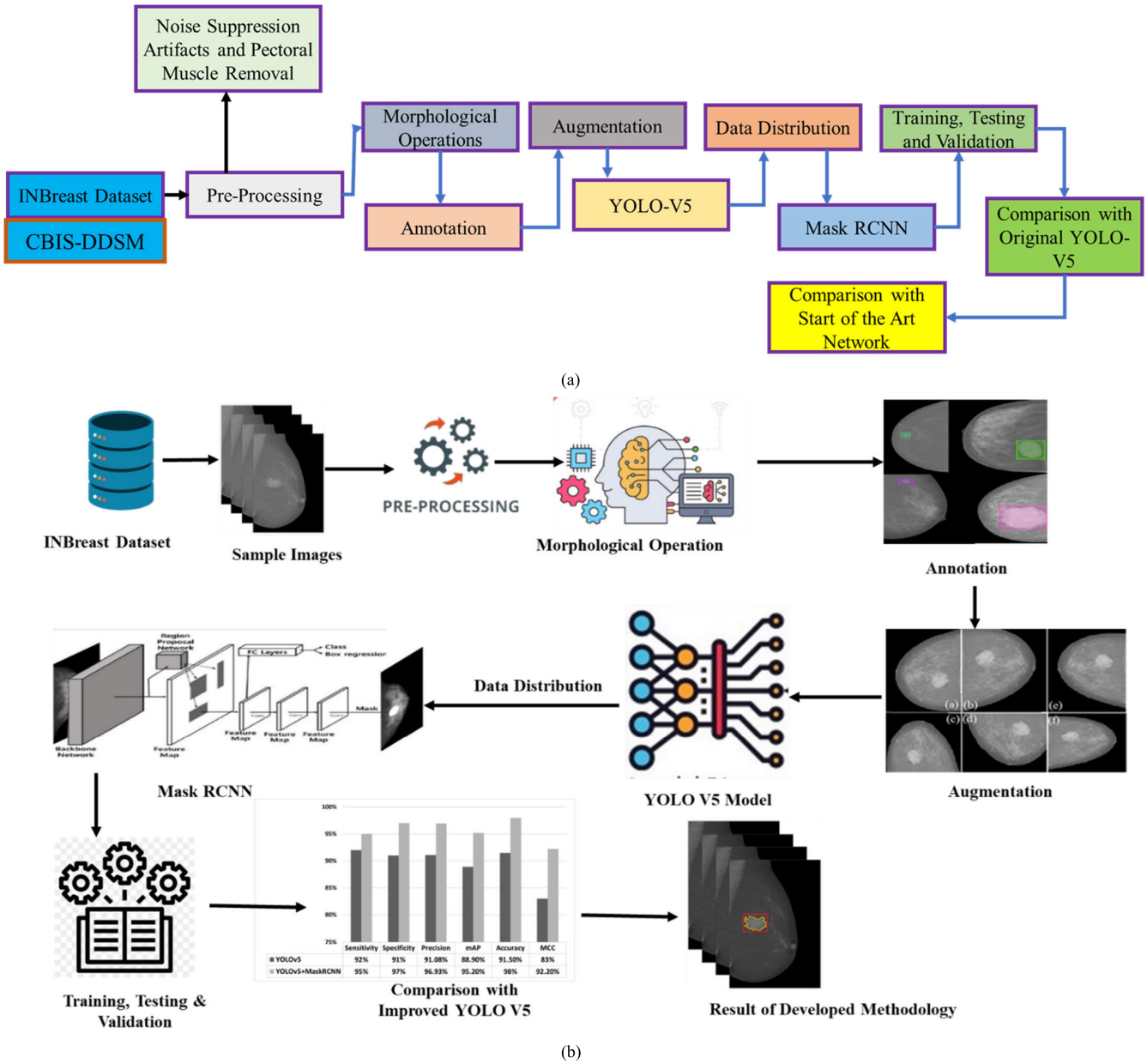

FIGURE 1. (a) Methodology block diagram. (b) Graphical representation of methodology block.

One potential drawback of this paper is that it may require big datasets for training and validating the network, which are not always easily accessible. The utilization of graph convolutional networks, which are able to successfully capture spatial and temporal relationships in sleep data, is the author's contribution in [28]. The model is quite flexible since domain generalization has been incorporated to make it more resilient across datasets. Graph convolutional networks have the potential to be quite resource intensive because to their computational complexity. In [29], the author makes a contribution by presenting a new neural network architecture tailored to the analysis of sleep EEG signals. Spiking neural networks are used, which is novel and fits well with the biological origins of EEG data. However, this strategy may struggle in contexts with limited resources because to the high computational requirements of training and deploying such networks.

III. METHODOLOGY

The objective of this endeavour is to automate the procedure of discerning the malignancy or benignity of an aberration in a mammography image that portrays a breast tumour. Figure 1(a) illustrates the overarching framework of the proposed strategy, while Figure 1(b) presents a graphical representation of the methodology block diagram. The utilisation of Contrast Limited Adaptive Histogram Equalization (CLAHE) as a preprocessing step is employed to enhance and refine mammograms. Superior results are attained with the

elimination of artefacts and pectoral muscles. Subsequently, the photos undergo the addition of BI-RADS annotations. The researchers utilised a method of augmentation to obtain more images for the purpose of enhancing the model-learning process. Subsequently, the data for detection and classification was provided to YOLOv5 and Mask RCNN, which are currently regarded as two of the most advanced models in existence. The Mask RCNN framework was employed to perform semantic segmentation, enabling the identification and description of the most prominent characteristics exhibited by the tumours included in the mammograms. The YOLOv5 model underwent a reduction in the fundamental parameters related to computing. The experiments were conducted using the same dataset to train the revised version. The improved performance of the model can be attributed to two factors: firstly, a reduction in complexity, and secondly, the incorporation of lightweight features. The outputs of both models are compared and contrasted. The objectives of this investigation encompass the prognostication and categorization of both benign and malignant tumours, with the mitigation of false positive rates (FPR) and false negative rates (FNR). The veracity of the findings is confirmed through rigorous testing. The effectiveness of the recommended model is examined by a comparative analysis with other similar studies, demonstrating that the proposed technique yields superior results in terms of Matthews Correlation Coefficient (MCC) [24]. The method described in this study presents radiologists with a practical approach to ascertain the classification, dimensions, and potential staging of a cancer. In the subsequent parts, we will delve into the particulars of the process.

A. DATASET DESCRIPTION

Experiments utilized a public INbreast (InBreast | Kaggle) and CBIS-DDSM dataset (https://www.kaggle.com/datasets/awsaf49/cbis-ddsm-breast-cancer-image-dataset) and BNS Dataset (http://cbio.mines-paristech.fr/~pnaylor/BNS.zip) with ground truth annotations. A total of 410 full-field digital mammograms (FFDMs) were obtained from a cohort of 115 women for the purposes of screening, diagnosis, and follow-up [27]. The experiment protected the patient's identity. Healthy, malignant, and noncancerous data are collected. It combines cranial-caudal (CC) and mediolateral-oblique (MLO) perspectives. Mammography diagnoses breast cancer. Malignant tumours have rough edges, are larger than surrounding tissue, and are whiter. As seen in Fig. 2, benign tumours are round or oval with sharp edges.

B. DATA PRE-PROCESSING

This study aims to automate mammography cancer detection for atypical breast lumps. Photos must be prepared. Preprocessing enhances desired features and reduces distracting artefacts to improve image quality. This study utilizes INbreast dataset. After removing background noise, Contrast Limited Adaptive Histogram Equalization CLAHE enhanced mammography contrast. Eliminating artefacts and pectoral

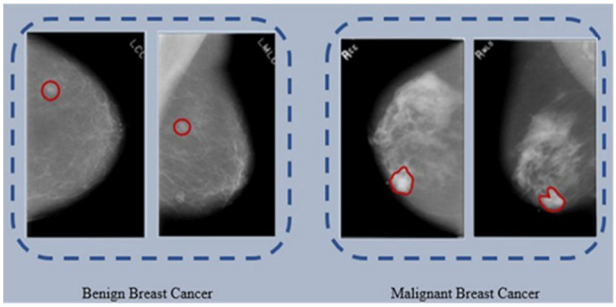

FIGURE 2. Benign and malignant breast tumor.

muscles improved results. CLAHE improved tumour visibility in mammography. CLAHE uses tiling. See the image in ''tiles'' instead of the whole thing. Two variables are needed for CLAHE to work. The first contrast-threshold value was 40. Second, the tile grid's rows and columns were specified. After that, the database's BI-RADS annotated the photos. These steps prepared the pictures for analysis: Median and mean filters denoise. The mammographic images were median and mean filtered to reduce noise and eliminate artifacts. Salt and pepper noise was reduced using the median filter yet sharp mammography edges were maintained. The median filter's false outlines were subsequently eliminated with the help of the mean filter. In the mediolateral oblique view (MLO) of mammograms, the pectoral muscles can obscure the tumor site, leading to a false positive. In order to properly identify the lesion, it is necessary to clear MLO views of artifacts and pectoral muscles. To do this, the mammographic pictures were altered by removing the pectoral muscles. The mammographic pictures were preprocessed with these methods before being sent into YOLOv5 for tumor detection and classification. Since tumors and breast parenchyma can be difficult to distinguish in complicated pictures, YOLOv5 was updated to improve its effectiveness in detecting and categorizing cancers. Parameters and model size were reduced by cutting off the convolutional layer from the Bottleneck CSP module's input feature map and directly connecting it to the output feature map. The salt-and-pepper noise and sharp edges in mammograms are initially preserved by using a median filter. Median filter equation could be written as

$$\mathbf{imgo(xi, yi) = med\{imgi(xi - \hat{J}, yi - k)j, k\epsilon T\}} \quad (1)$$

where imgo(xi,yi)is the output and imgi(xi,yi) are the input operated images, respectively, and j and k denote the pixels in the image, the 2-dimensional mask has dimensions of n x n as depicted in Eq(1). The median filter could produce spurious outlines, which could then be removed using the mean filter.

C. PECTORAL MUSCLE DELETION

The pectoral muscles are visible in the mammographic images when viewed in the mediolateral oblique (MLO) position. Mammographic images show them alongside breast parenchyma since their intensity values are the same. This could result in an incorrect diagnosis of the tumor's location.

Because of this, accurate lesion identification relies on MLO views being processed to exclude artefacts and pectoral muscle as shown in figure 3.

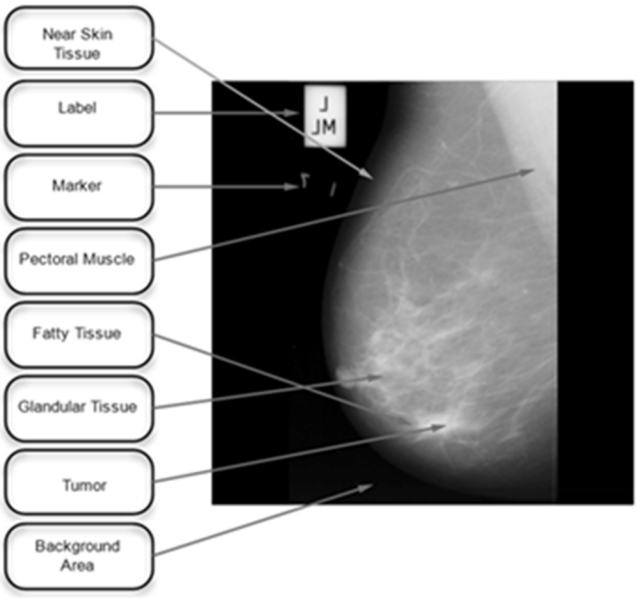

FIGURE 3. Pectoral muscle and breast tissue.

Figure 4 presents the results both before and after the mammograms were preprocessed.

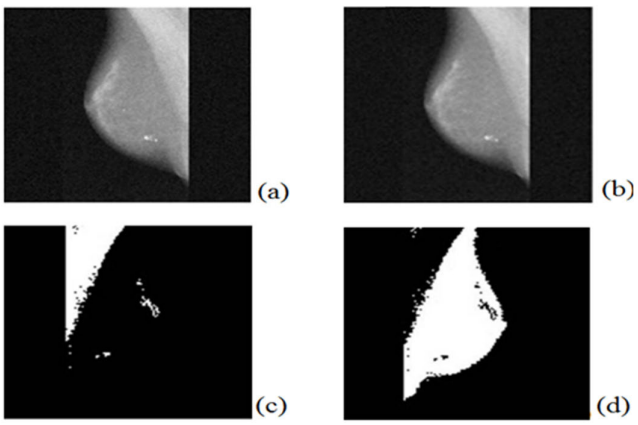

FIGURE 4. (a) Original image (b)denoised image (c) identified pectoral region using global threshold (d) pectoral muscle removal using global and gray level threshold.

D. ANNOTATIONS

Annotation labels create meaningful annotated mammographic images. Both algorithms utilize marked data. Mask RCNN semantic segmentation. It distinguishes tumour types. Malignant tumours have jagged edges, while benign ones are smooth. Two files hold data annotations. Mammogram images and bounding box dimensions are in.jpg and.txt files, respectively. Annotated picture file in Figure 5. The XML file shows histological evidence of the lesions. Radiologists classify tumours using BI-Rads. The 107 instances include 41 BI-RAD 2 or 3 masses and 75 BI-RAD 4, 5, or 6 malignant masses.

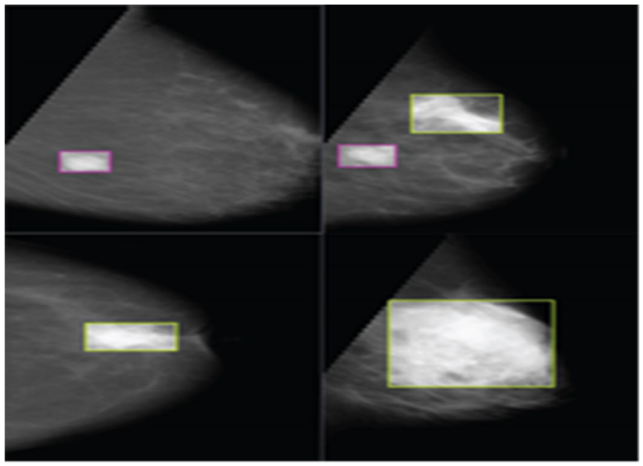

FIGURE 5. Annotated images.

E. DATA AUGMENTATION

Data augmentation purposefully alters photographs to enlarge the dataset and training model. It lets the model learn to intentionally absorb features for better object discrimination. 107 lesioned mammograms were utilised to train and test the model. Some breasts had several masses. 116 masses result. Fig. 6 shows how data augmentation can increase training data sample size and model performance.

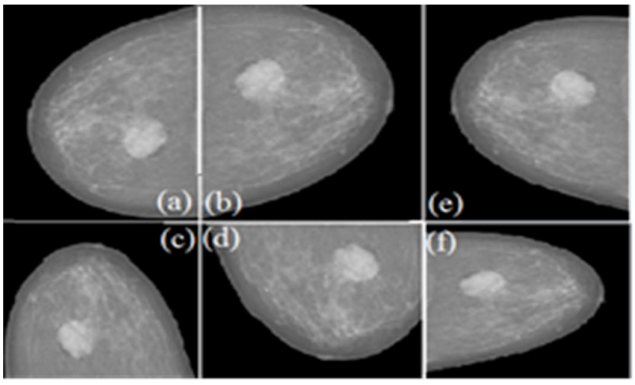

FIGURE 6. Augmentation of data.

F. YOLOv5 ARCHITECTURE

YOLOv5 is a neural network that employ deep learning to recognize and categorize objects. This study employs the use of mammography images to distinguish between benign and malignant tumours. Both melanoma and melanocytic nevus can be recognised efficiently due to the end-to-end nature of the process [29]. It makes use of global features and copes effectively with unexpected inputs. Thus, YOLO can play this role. Mass detection begins by drawing a bounding box around the abnormality on the input image to classify it as benign or malignant. YOLO architecture has three main parts 31. YOLOv5 Backbone, Neck, and Head (Figure 7). Bottleneck CSP, designed for feature extraction,

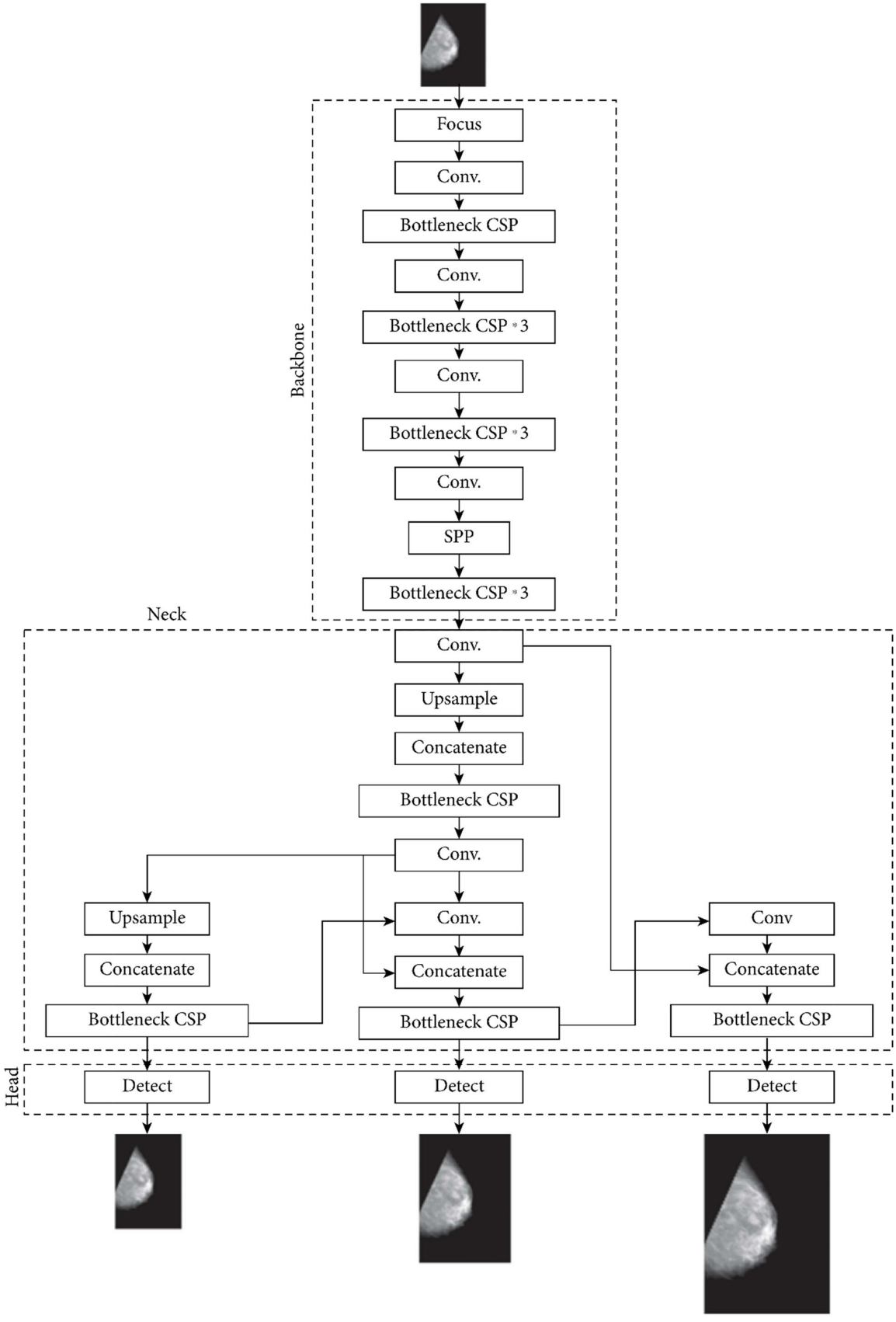

FIGURE 7. YoloV5 architecture.

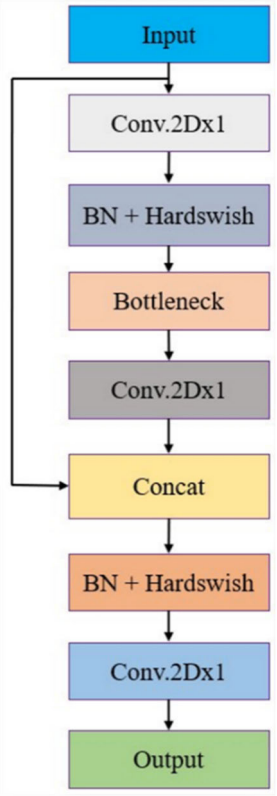

FIGURE 8. Bottleneck CSP improved architecture.

is YOLOv5's central model. The proposed methodology utilizes improved yolov5 although YOLOv5 model is fast and efficient, it may have trouble predicting and classifying lesions in particularly complicated pictures where the distinction between tumors and breast parenchyma is blurry. The YOLOv5 main model is quite sophisticated, with many convolutional layers spread throughout its four Bottleneck CSP modules. While this may result in more accurate feature extraction, the larger model and associated implementation challenges are a result of the greater number of parameters. Thus, the model is enhanced by tweaking the skeleton in order to cut down on parameter and overall model size. The initial backbone layer requires fewer calculations, speeding up training. Slices the three-image into four 320 × 320 × 3 parts. The second backbone layer's 32-convolution kernel layer merges the four segments' output feature maps into a 12 × 320 × 320 map. With Batch Normalization, the data is processed further (BN). Level 3 of the structural backbone adds a 3 × 3 convolution layer to Bottleneck CSP's 1 × 1 (Conv2d layer, Batch Normalization, and ReLu). When combined, Bottleneck yields the following:

$$A1 = B1 \times A0 \tag{2}$$

$$A2 = B2 \times [A0, A1] \tag{3}$$

$$AK = Bk \times [A0, A1, \ldots, Ak - A1]. \tag{4}$$

where [A0, A1....] represents the concatenation in Eq(2, 3), Bk represents the layer weights, and Ak represents the k-th layer's output in Eq (4). As a result, the dimensions of the output feature map end up matching those of the input. The YOLOv5 model incorporates PANet in its neck architecture to generate feature pyramids, which effectively enhances the model's performance by lowering runtime and streamlining the overall process [27]. It helps the model function well when faced with unexpected data. The YOLOv5 model's brain was built with final detection in mind. It's made up of three distinct layers. Each of the three levels has a size of 80 × 80, 40 × 40, and 20 × 20. Different sized images are located employing anchor boxes that contain class probabilities, objectless scores, and bounding boxes. G. Improvement & enhancements to YOLOv5 The YOLOv5 model is fast and accurate, but it has trouble distinguishing cancers from breast parenchyma in images. The basic model has many convolutional layers and four Bottleneck CSP modules, making it difficult. Increasing the model's parameters makes hardware implementation harder, but it can extract features with high accuracy. This research improves the foundational model. The Bottleneck CSP module's input feature map was coupled to the model's output feature map to reduce input parameters and model size. Convolutional layer removed from branch. Figure 9 contrasts YOLOv5 backbone module variants. Modifying Bottleneck CSP modules may reduce parameters but reduce deep feature extraction efficiency. Equation 5 can calculate damage.

$$C = P(\text{tumor}) \times \text{lossp} \tag{5}$$

$$IOU = \text{area}(BP \cap Bgt)/\text{area}(BP \cup Bgt) \tag{6}$$

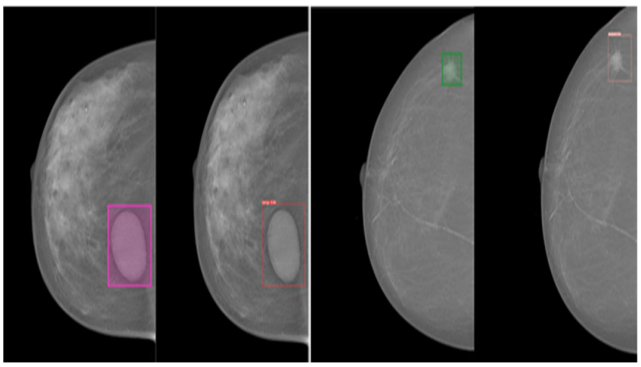

FIGURE 9. Benign & malignant input and output image.

The loss-calculating function is depicted by Equation (5). The probability that the grid cell in question contains a tumor is denoted by P (Tumor), and the confidence level is denoted by C as depicted in Eq(5). If the target's center is inside a grid cell during training, the value is 1. The default value is zero. The loss value is the difference between the true bounding box of a grid cell and the predicted bounding box. Commonly employed to quantify the degree to which two boxes coincide, IoU stands for "the junction and unity of two boxes." Equation (6) demonstrates the calculation procedure. The probability of a tumor's presence, denoted by the symbol P(tumour), is given by C = (tumour) / (confidence). To determine lossp, the difference between the predicted

bounding box and the ground truth box is calculated and assigned a value based on whether or not the tumor's center is located within the cell grid (P = 1). The degree of overlap between two detection frames is measured by the IOU, which is given by the equation (6). the projected frame Bp and the actual frame Bgt.H. Mask RCNN Based on Faster-RCNN 16, Mask-RCNN detects object shape using pixel-by-pixel approximation and segmentation mask predictions for each Area of Interest (RoI).

The convolutional neural network (CNN) is capable of generating object bounding boxes, class labels, and confidence ratings by using regions. The term ''mask'' refers to a covering that is worn over the face, typically made The RCNN model employed in this context follows a two-stage approach. Submission of Initial Proposal At the outset, a backbone network such as Inception or ResNet, along with a region proposal network (RPN), is utilised. The backbone algorithm establishes the delineation of the region of interest (ROI), while the region proposal network (RPN) proposes a potential site of a tumour inside the delineated ROI. Anchor boxes are utilised to accurately locate objects. The algorithm produces suggested geographical areas on a single occasion for each image. The proposed regions inside the feature map encompass the item.

Stage 2: Anticipatory Analysis The bounding boxes and item classes of the proposed regions are predicted through the utilisation of a two-pass RCNN detection method. To ensure the preservation of a uniform region size, researchers may opt to utilise the RoI Align technique or RoI pooling approach. Tumour Size Prediction As previously said, early detection of illnesses serves as a preventive measure. Initially, the tumour is of such diminutive proportions that it is imperceptible. The entity undergoes expansion, infiltrates the dermal parenchyma, and assumes a spiky morphology. According to the findings presented in Table 1, tumours measuring between 20mm and less than 50mm in diameter exhibit a higher likelihood of successful treatment compared to tumours measuring 50mm or more. This observation implies the presence of metastatic malignancy in the latter group. The model is trained using a Mask RCNN. Figure 8 illustrates the reception of the image by the core processing network of the Convolutional Neural Network (CNN). While ROI Align generates ROI features, the Region Proposal Network (RPN) identifies and delineates them. The RCNN and Mask heads estimate Mask Intersection over Union using the expected mask and ROI features. MaskIoU Head has four convolutional and three completely connected layers. Mask Intersection over Union class outputs come from the last fully connected layer. Detecting the condition early prevents it. At first, a tumor is invisible. The item expands, penetrates the skin's parenchyma, and is spiky. Metastatic malignancy is indicated by lesions beyond 50 mm, although those 20–50 mm can be treated. Breast cancer staging, created in 2–5, ranks tumors by aggressiveness [25]. The model was trained using mask RCNN. The Mask RCNN algorithm segments mammography tumors and identifies those that need additional scrutiny. The two-category dataset uses semantic segmentation.

Both YOLOv5 and Mask RCNN used methodical approaches during their training processes. Contrast Limited Adaptive Histogram Equalization (CLAHE) was used in the preprocessing step of YOLOv5 to improve mammography and remove artifacts. To improve the dataset, data augmentation techniques were used. To test the model's performance, it was trained on a variety of resolutions (440×448, 640×648, and 832 × 832). In order to make YOLOv5 more efficient, especially in differentiating cancers from breast parenchyma, we reduced some of its parameters. Metrics for evaluation included things like recall, average precision percent, precision, true positives, and false positives.

Mask RCNN used semantic segmentation to define and identify tumor features. To ensure a fair comparison, the dataset and preprocessing processes were in line with YOLOv5. Considering the importance of early detection, Mask RCNN was trained for precise tumor identification and its capacity for tumor size prediction was studied. Mask Intersection over Union (MaskIoU) was one of the metrics used to evaluate Mask RCNN. These approaches sought to enhance breast tumor identification and categorization by focusing on aspects including model efficacy, precision, and the capacity to manage complex mammography images.

Subsequently, edge contours are extracted from the entirety of the mass in order to build the most compact bounding box for each individual mass. Finally, the bounding box provides an estimation of the volume of the tumour. This therapeutic intervention demonstrates efficacy in addressing even the most atypical neoplasms. The Python programming language is capable of making size predictions.

TABLE 1. YOLO-V5+Mask RCNN on augmented datasets.

Terms	*Augmentation Approach 1*	*Augmentation Approach 2*
B: TP-FP	4-2	26-1
M: TP-FP	11-0	62-1
B: AP%	76.7	96.3
M: AP%	75.1	98.4
Precision	88	98
Recall	62	99
mAP (%) IOU-0.5	76.8	97.4

IV. EXPERIMENTATION

In the dataset, 60% of the total 2120 mammograms are allocated for model training, while 30% are reserved for validation purposes, and the remaining 10% are designated for testing. The web-based markup tool, Makesense.ai, was utilised to assign labels to photos, categorising them as either benign or malignant, and also providing a boundary in the form of a rectangle. The bounding box of the lesion is labelled by mammographers. The augmentation technique was used solely to the training data. The primary objective of this

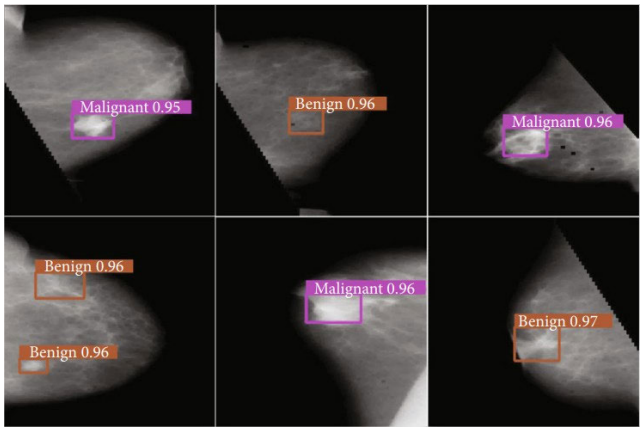

FIGURE 10. Identified and categorized breast tumours.

technique is to modify the images in the training set during the training process, so enabling the model to acquire knowledge of a wide range of conceivable scenarios. Therefore, the test dataset was not subjected to augmentation. The model's training on the augmented dataset provided confirmation of this finding. The original data set was augmented and divided into two separate test sets. Another strategy that was employed involved the division and enhancement of the training data. The second iteration exhibits much higher mean Average Precision (mAP) values. The present investigation utilised the second approach.

Figures 9 present visuals that depict both input and output for benign and Malignant Image. The pixel values of the mammography, ranging from 0 to 214 with a contrast of 14 bits, can be converted into a total of 16,384 values when scaled to a range of 0 to 255. The lesion coordinates and ground truth annotations of the XML file are normalised within the range of [1, 0], with respect to the height and width of the image. The parameters are preserved for the purpose of training subsequent photographs. Simulations utilise scaled mammograms. The models were trained at three different resolutions: 440 × 448, 640 × 648, and 32 × 832. Conducting training on the baseline model followed by the upgraded version using same data can be employed to assess the effectiveness of the modified version. This analysis aims to compare the outcomes of both models. This study involves the training of the YOLOv5 model utilising a series of experimental scenarios.

V. RESULTS

The MCC metric is often regarded as the most effective measure for evaluating binary classification ability. The maximum value of the confusion matrix is attained when all four parameters are accurately predicted. The average accuracy of the model holds significance. This metric assesses the effectiveness of system training. Based on the available data, it can be observed that the revised model resulted in a notable increase of 0.092 in the Matthews Correlation Coefficient (MCC) value. The validation of the model's enhanced performance across all four parameters, namely True Positive

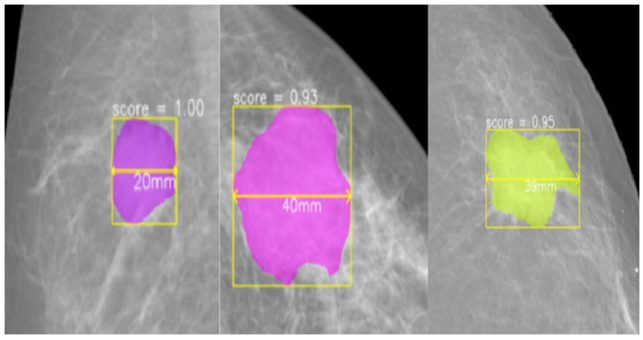

FIGURE 11. Breast tumor size prediction.

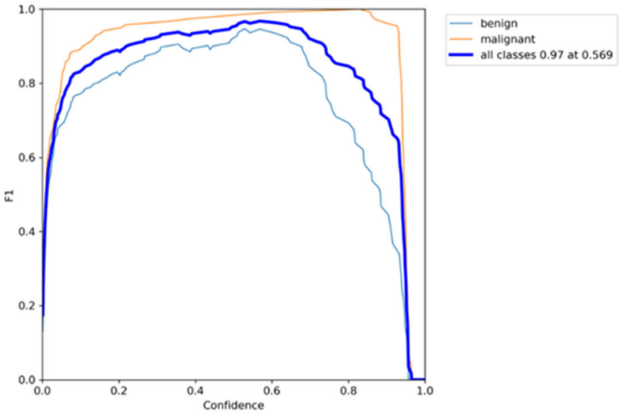

FIGURE 12. F1 score for dataset.

Rate (TPR), True Negative Rate (TNR), False Positive Rate (FPR), and False Negative Rate (FNR), is evident. When assessing the efficacy of the model, various metrics are used. The performance metric parameters are given below from Eq (7) to Eq(15), as shown at the bottom of the next page, where Eq(7) shows sensitivity, Eq(8) shows precision, Eq(9) shows Accuracy, Eq(10) presents specificity, Eq(11) shows mAp, Eq(12) shows False negative rate, Eq(13) shows False positive rate, Eq(14) presents Mathew Correlation coefficient, and Finally Eq(15) presents F-measure.

According to the findings presented in Figure 10, it can be observed that the model, which underwent suitable training, had the capability to detect and classify breast masses. The ease of the model in recognizing and classifying the breast mass is depicted in Figure 10. The estimations regarding the size of the tumour were accurate as well. Figure 11 displays three instances of malignancy. Figure 12 depicts a malignancy of 20mm, accompanied by two more stage 3 tumours measuring 40mm and 39mm, respectively. The F1 score can be defined as the harmonic mean of the Precision and Recall metrics. The method takes into consideration both false positives and false negatives. The F score exhibits greater precision compared to accuracy, particularly in scenarios where there is an unequal distribution of classes. However, comprehending the F score can be more challenging. The highest level of accuracy is achieved when the number of false positives and false negatives are equal. According to

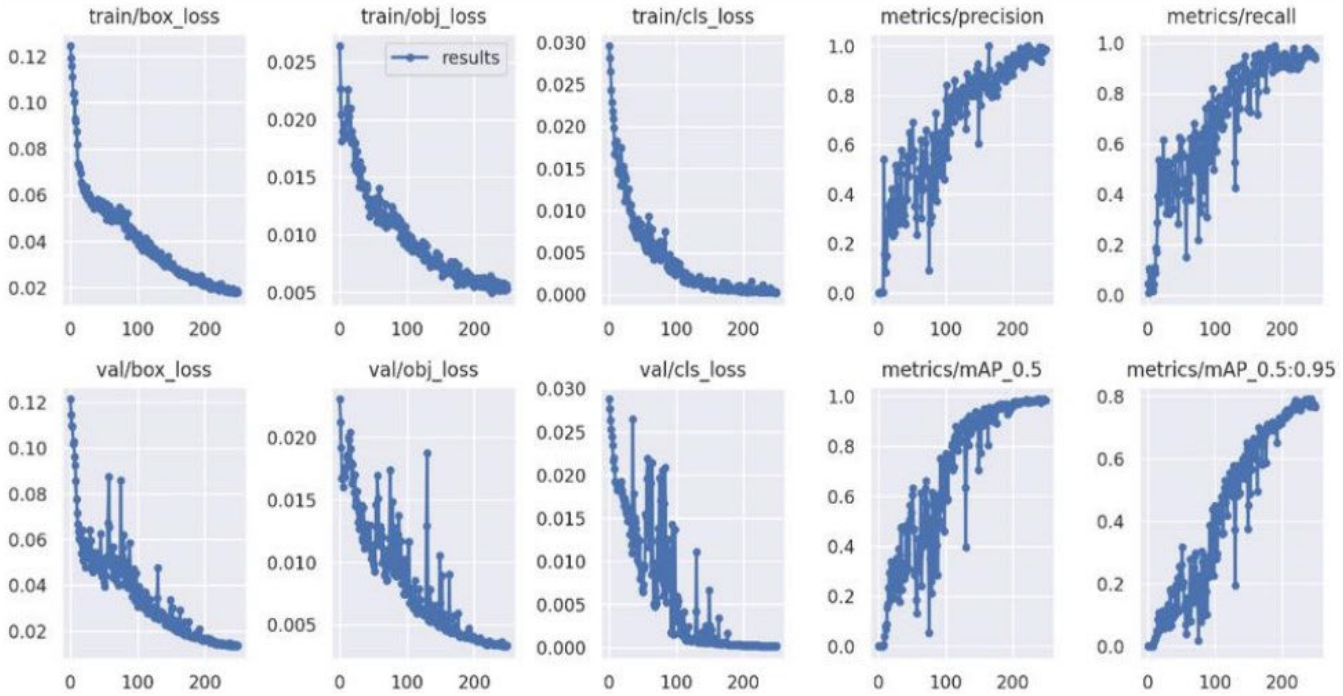

FIGURE 13. Training and validation processes loss.

Figure 12, the range of ideal F1 scores lies between 0.6 and 0.9.

Model performance is depicted in Figure 13. The observed IOU loss during both the training and validation stages indicated that the model achieved its optimal performance at epoch 200. Overfitting is observed beyond this threshold. The present study employed a Python 3.6 implementation of the cutting-edge algorithms YOLOv5 and Mask RCNN to perform the generalization of the work, specifically for the purpose of identifying and categorizing mammography masses. Tumours are classified based on their size. The data for training, validation, and testing purposes was distributed in a random manner. Only the training set was subjected to augmentation. The testing data was not observed during the training phase. The experiment utilised a learning rate of 0.0010 and a decay rate of 0.999 each iteration. A LR model with limited complexity is trained. The ROC curve visually represents the relationship between the true positive rate, also known as sensitivity, and the false positive rate, which is the complement of specificity, across different thresholds for a specific parameter.

Once a decision threshold is determined, each point on the Receiver Operating Characteristic (ROC) curve indicates a mix of sensitivity and specificity, as seen in Figure 14. The experimental results presented in Figure 15 demonstrate that the utilisation of modified YOLOv5 in combination with Mask RCNN leads to a notable increase in the MCC value, rising from 83% to 92%. The observed decrease in the false

$$Sensitivity = {TP}/{TP + FN} \tag{7}$$

$$precision = {TP}/{TP + FP} \tag{8}$$

$$Accuracy = {TN + TP}/{FP + TN + TP + FN} \tag{9}$$

$$Specificity = {TN}/{FP + TN} \tag{10}$$

$$mAp = \frac{1}{N}\sum_{i=1}^{N} APi \tag{11}$$

$$FNR = 1 - Sensitivity = {FN}/{TP + FN} \tag{12}$$

$$FPR = 1 - Specificity = {FN}/{TP + FN} \tag{13}$$

$$MCC = {(TP)\,(TN) - (FP)(FN)}\Big/{\sqrt{(TP + FP)(TP + FN)(TN + FP)(TN + FN)}} \tag{14}$$

$$F - Measure = {2(sensitivity)(Precision)}/{Sensitivity + Precision} \tag{15}$$

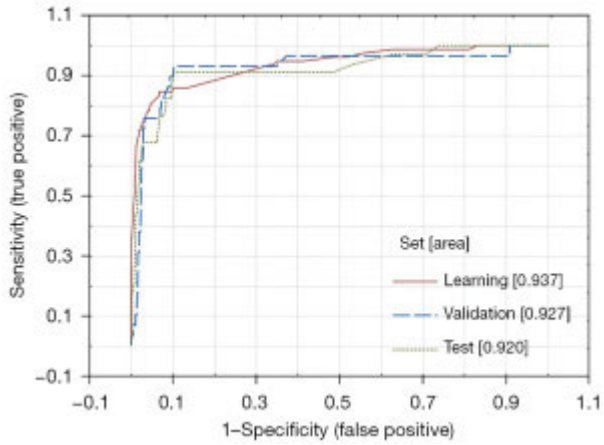

FIGURE 14. Receiver operating characteristics curve analysis.

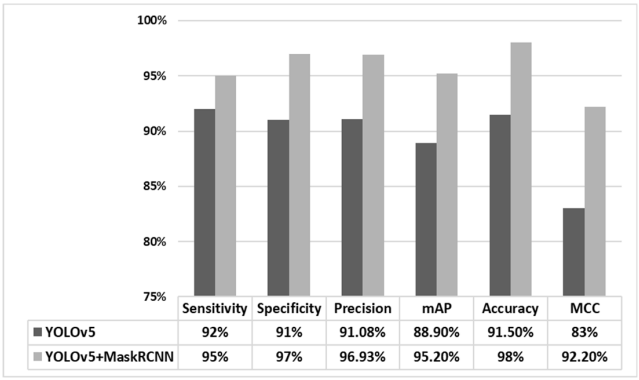

	Sensitivity	Specificity	Precision	mAP	Accuracy	MCC
YOLOv5	92%	91%	91.08%	88.90%	91.50%	83%
YOLOv5+MaskRCNN	95%	97%	96.93%	95.20%	98%	92.20%

FIGURE 15. Result comparison of YOLOV5 with improved YOLOV5.

positive rate (FPR) value is likewise statistically significant. Both the original and revised versions exhibit a False Positive Rate of 0.06 and a False Negative Rate of 0.03, respectively. There has been a significant improvement in precision, with the accuracy rate rising from 91.50% to 98%. Figure 16 illustrates the contrast between the suggested methodology and the current literature.

Similarly, the result utilized for BSN dataset are given below.

The neural network underwent training using the stochastic gradient descent (SGD) optimisation algorithm. The hyperparameters employed in this investigation were as follows: The training process consisted of 20,000 iterations, with a maximum number of epochs set to 200. The learning rate used was 0.01, and a batch size of 8 images was employed. The system under consideration is equipped with an Nvidia 1080-ti graphics processing unit (GPU), 16 gigabytes of random access memory (RAM), and an Intel i7 central processing unit (CPU). The enhancement in our model's performance during the training process may be observed in Figures 17 and 18. Plots depicting the precision and loss metrics throughout training epochs are available for both the training and validation datasets. The automated identification of cellular nuclei is an essential undertaking for deep learning-based methodologies. Figure 19 illustrates the outcomes of lesion

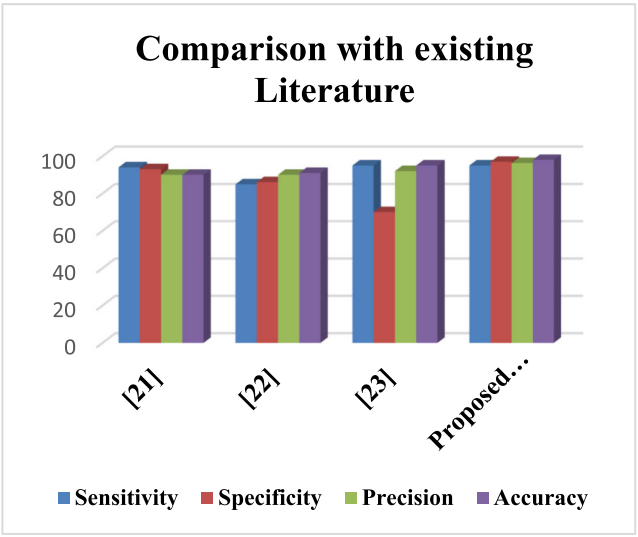

FIGURE 16. Result comparison with existing literature.

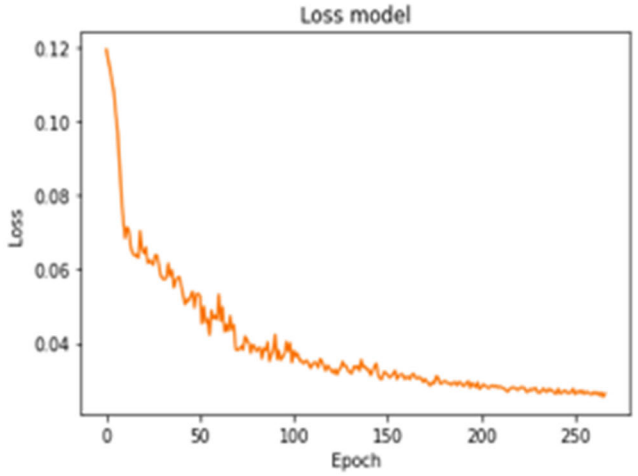

FIGURE 17. The training-period loss plot per epochs.

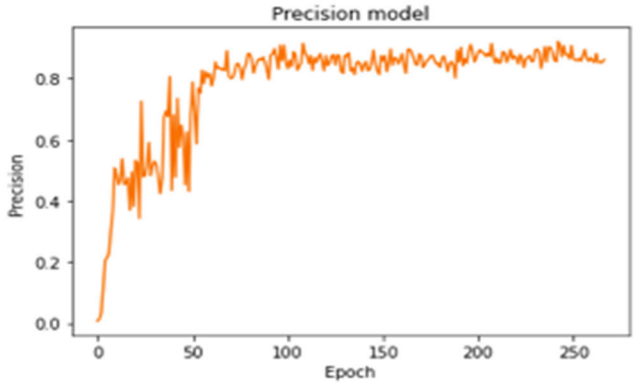

FIGURE 18. Accuracy as a function of time during training.

detection obtained from a specific dataset. Subfigure (a) displays the original images extracted from the test set, whereas subfigure (b) exhibits the detection findings achieved using the YOLOv5 algorithm.

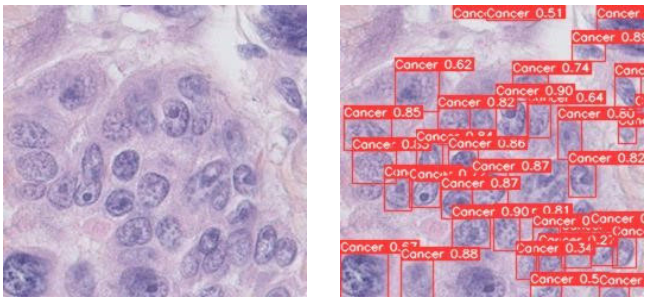

FIGURE 19. Detection result and images from the dataset.

Following the completion of the training process, the network was chosen based on its precision with respect to the validation set. Subsequently, the detection performance of the selected network was assessed using the test set. The object detection model achieved a precision of 0.86 and a recall of 0.77. The findings are presented in ''Table 2''.

TABLE 2. Metrics results.

Model	Metrics	
	Precision	*Recall*
YOLOv5	0.86	0.77

VI. CONCLUSION AND FUTURE WORKS

The objective of this study was to develop a deep learning model that can accurately detect and classify breast masses at an early stage, as well as assess the aggressiveness of malignant tumours. The introductory section provides an overview of breast anatomy, the historical development of Computer-Aided Diagnosis (CAD) software, and the many forms of breast cancer. This section provides an overview of the techniques employed by radiologists. The historical development of Computer-Aided Diagnosis (CAD) software, as well as its application in the healthcare sector, are also addressed. This section aims to provide a comprehensive assessment of recent research and machine learning methodologies. In order to detect the missing data, a comparison and assessment of the available data is conducted. The paper titled ''Datasets and Data Processing'' provides an overview of the INbreast dataset and outlines the steps taken to prepare it for training a model. Preprocessing filters are employed to eliminate muscular artefacts and noise. The inclusion of additional data resulted in an increase in the size of the dataset. Two steps are proposed. The initial step entails modifying the detection algorithm. This section provides a comprehensive overview of the internal workings of our proposed YOLOv5 algorithm. The scope of this study encompasses the examination of brain, neck, and spine functionality. The computations and footprint of the model are simplified. The concatenation layer receives data that has been bypassed from an additional convolution layer. The architectural components of the model are depicted. The efficacy of the model exhibited a decline in tandem with the reduction in its footprint and the overall number of calculations performed. The Mask RCNN method demonstrates the higher performance of the model. The subsequent analysis delves into the intricacies of Mask RCNN and semantic segmentation. The Mask RCNN algorithm is utilised to calculate the mass of tumours. The stage of cancer is determined by the size of the tumour. Therefore, the YOLOv5+Mask RCNN model utilises anchor boxes derived from mammographic images to accurately forecast the type of mass and accurately pinpoint the tumour. Breast lumps are assessed in terms of their dimensions and potential for cancer. The assessment of tumour aggressiveness is facilitated through the utilisation of image analysis techniques. The process of max pooling involves passing the output of one algorithm as input to another algorithm. The experimental section provides a comprehensive description of the preparation process for the INbreast Dataset. The photographs were annotated by an expert to indicate the presence of tumours. The process of categorising data into bonding boxes, distinguishing between healthy and malignant data. The XML file contains data on tumours that have been scored using the BI-RAD scoring system. In order to comprehend augmentation approaches, researchers initially enhanced the datasets used for training and testing purposes. Subsequently, solely the test dataset was expanded. A comparison was made between both strategies. In order to ensure reproducibility, we provide a comprehensive set of model training settings, assessment metrics, graphs, outcomes, and experimental figures. The accuracy and Matthews Correlation Coefficient (MCC) value demonstrated improvement. The combined utilisation of the hybrid innovative methodology, specifically the integration of YOLOv5 and Mask RCNN, demonstrated superior performance compared to individual detection approaches. The utilisation of this technique has the potential to enhance the efficiency of radiologists' decision-making processes, as it involves the validation of findings by an expert in the relevant field. The incorporation of supplementary models alongside YOLOv5 to enhance the Matthews Correlation Coefficient (MCC) has the potential to yield intriguing outcomes. These models may also exhibit high performance on 3D mammography.

DATA AVAILABILITY

The data would be available upon special request to the corresponding author via email.

REFERENCES

[1] *GLOBOCAN 2020: New Global Cancer Data | UICC*. Accessed: Sep. 29, 2021. [Online]. Available: https://www.uicc.org/news/globocan-2020-new-global-cancer-data

[2] S. M. Lima, R. D. Kehm, and M. B. Terry, ''Global breast cancer incidence and mortality trends by region, age-groups, and fertility patterns,'' *eClinicalMedicine*, vol. 38, Aug. 2021, Art. no. 100985.

[3] A. Muhammad, M. Javed, and R. Hamid, ''Breast cancer in Pakistan: Alarming situation of breast cancer in near future,'' *Iranian J. Public Health*, vol. 49, no. 4, pp. 812–813, Apr. 2020.

[4] S. Saeed, M. Asim, and M. M. Sohail, "Fears and barriers: Problems in breast cancer diagnosis and treatment in Pakistan," *BMC Women's Health*, vol. 21, no. 1, p. 151, Dec. 2021.
[5] G. Zucca-Matthes, C. Urban, and A. Vallejo, "Anatomy of the nipple and breast ducts," *Gland Surg.*, vol. 5, no. 1, pp. 32–36, Feb. 2016.
[6] S. Zahoor, I. U. Lali, M. A. Khan, K. Javed, and W. Mehmood, "Breast cancer detection and classification using traditional computer vision techniques: A comprehensive review," *Current Med. Imag. Formerly Current Med. Imag. Rev.*, vol. 16, no. 10, pp. 1187–1200, Jan. 2021.
[7] A.-K. Vranso West, L. Wullkopf, A. Christensen, N. Leijnse, J. M. Tarp, J. Mathiesen, J. T. Erler, and L. B. Oddershede, "Division induced dynamics in non-invasive and invasive breast cancer," *Biophysical J.*, vol. 112, no. 3, p. 123a, Feb. 2017.
[8] S. Iranmakani, T. Mortezazadeh, F. Sajadian, M. F. Ghaziani, A. Ghafari, D. Khezerloo, and A. E. Musa, "A review of various modalities in breast imaging: Technical aspects and clinical outcomes," *Egyptian J. Radiol. Nucl. Med.*, vol. 51, no. 1, p. 57, Dec. 2020.
[9] J. Y. Jang, S. M. Kim, J. H. Kim, M. Jang, B. La Yun, J. Y. Lee, S. H. Lee, and B. Kim, "Clinical significance of interval changes in breast lesions initially categorized as probably benign on breast ultrasound," *Medicine*, vol. 96, no. 12, p. e6415, Mar. 2017.
[10] (2020). *Diagnosis, B.C.E.D.A. Limitations of Mammogram*. Accessed: Jan. 1, 2023. [Online]. Available: https://www.cancer.org/cancer/types/breast-cancer/screening-tests-and-early-detection/mammograms/limitations-of-mammograms.html
[11] S. P. Mohanty, D. P. Hughes, and M. Salathé, "Using deep learning for image-based plant disease detection," *Frontiers Plant Sci.*, vol. 7, p. 1419, Sep. 2016.
[12] T. Hazra and K. Anjaria, "Applications of game theory in deep learning: A survey," *Multimedia Tools Appl.*, vol. 81, no. 6, pp. 8963–8994, Mar. 2022.
[13] D. A. Ragab, O. Attallah, M. Sharkas, J. Ren, and S. Marshall, "A framework for breast cancer classification using multi-DCNNs," *Comput. Biol. Med.*, vol. 131, Apr. 2021, Art. no. 104245.
[14] J. C. Bailar, "Mammography: A contrary view," *Ann. Internal Med.*, vol. 84, no. 1, pp. 77–84, Jan. 1976.
[15] M. Aaqib, M. Tufail, and S. Anwar, "A novel deep learning based approach for breast cancer detection," in *Proc. 13th Int. Conf. Math., Actuarial Sci., Comput. Sci. Statist. (MACS)*, Dec. 2019, pp. 1–6.
[16] C. Eyupoglu, "Breast cancer classification using k-nearest neighbors algorithm," *Online J. Sci. Technol.*, vol. 8, no. 3, pp. 29–34, 2018.
[17] S. Abbas, Z. Jalil, A. R. Javed, I. Batool, M. Z. Khan, A. Noorwali, T. R. Gadekallu, and A. Akbar, "BCD-WERT: A novel approach for breast cancer detection using whale optimization based efficient features and extremely randomized tree algorithm," *PeerJ Comput. Sci.*, vol. 7, p. e390, Mar. 2021.
[18] G. Meenalochini and S. Ramkumar, "Survey of machine learning algorithms for breast cancer detection using mammogram images," *Mater. Today, Proc.*, vol. 37, pp. 2738–2743, Jan. 2021.
[19] H. B. Lim, N. T. T. Nhung, E.-P. Li, and N. D. Thang, "Confocal microwave imaging for breast cancer detection: Delay-multiply-and-sum image reconstruction algorithm," *IEEE Trans. Biomed. Eng.*, vol. 55, no. 6, pp. 1697–1704, Jun. 2008.
[20] K. Iftikhar, S. Anwar, I. U. Haq, M. T. Khan, and S. R. Akbar, "An optimal neural network based classification technique for breast cancer detection," *J. Eng. Appl. Sci.*, vol. 35, no. 1, pp. 51–58, 2016.
[21] M. R. Joshi, L. Nkenyereye, G. P. Joshi, S. M. R. Islam, M. Abdullah-Al-Wadud, and S. Shrestha, "Auto-colorization of historical images using deep convolutional neural networks," *Mathematics*, vol. 8, no. 12, p. 2258, Dec. 2020.
[22] D. A. Ragab, M. Sharkas, and O. Attallah, "Breast cancer diagnosis using an efficient CAD system based on multiple classifiers," *Diagnostics*, vol. 9, no. 4, p. 165, Oct. 2019.
[23] M. Diwakar, P. Sharma, S. Swarnakar, and P. Kumar, "Image security using cellular automata rules," in *Proc. 3rd Int. Conf. Soft Comput. Problem Solving (SocProS)*, vol. 1. Cham, Switzerland: Springer, 2014, pp. 403–412.
[24] C. Singla, P. K. Sarangi, A. K. Sahoo, and P. K. Singh, "Deep learning enhancement on mammogram images for breast cancer detection," *Mater. Today, Proc.*, vol. 49, pp. 3098–3104, Dec. 2022.
[25] O. Attallah, F. Anwar, N. M. Ghanem, and M. A. Ismail, "Histo-CADx: Duo cascaded fusion stages for breast cancer diagnosis from histopathological images," *PeerJ Comput. Sci.*, vol. 7, p. e493, Apr. 2021.
[26] H.-W. Ting, S.-L. Chung, C.-F. Chen, H.-Y. Chiu, and Y.-W. Hsieh, "A drug identification model developed using deep learning technologies: Experience of a medical center in Taiwan," *BMC Health Services Res.*, vol. 20, no. 1, p. 312, Dec. 2020.
[27] Z. Jia, Y. Lin, J. Wang, X. Wang, P. Xie, and Y. Zhang, "SalientSleepNet: Multimodal salient wave detection network for sleep staging," May 2021, *arXiv:2105.13864*.
[28] Z. Jia, Y. Lin, J. Wang, X. Ning, Y. He, R. Zhou, Y. Zhou, and L. H. Lehman, "Multi-view spatial–temporal graph convolutional networks with domain generalization for sleep stage classification," *IEEE Trans. Neural Syst. Rehabil. Eng.*, vol. 29, pp. 1977–1986, 2021.
[29] Z. Jia, J. Ji, X. Zhou, and Y. Zhou, "Hybrid spiking neural network for sleep electroencephalogram signals," *Sci. China Inf. Sci.*, vol. 65, no. 4, Apr. 2022, Art. no. 140403.

MUHAMMAD ANAS received the master's degree in electrical engineering from the University of Gujrat, Hafiz Hayat Campus, Gujrat, Punjab, Pakistan. He is working as a Lecturer with TEVTA Punjab.

IHTISHAM UL HAQ received the bachelor's degree in mechatronics engineering, and the master's degree in automation and control from University of Engineering and Technology (UET) Peshawar, in 2022, showcasing his commitment to continuous learning and growth. Currently, he is pursuing the Ph.D. degree with the prestigious Mechatronics Department, where he is delving deeper into the captivating realms of clinical image processing, artificial intelligence, machine learning, deep learning, and eXplainable AI. His bachelor's degree laid the strong foundation for his academic pursuits. He is a passionate and dedicated Researcher. He is also a Research Associate with NCAI UET, Peshawar, where his journey in academia began as a Research Assistant, from June 2021 to June 2022. He honed his skills and nurtured his curiosity for cutting-edge technologies with NCAI UET. Prior to that, he contributed his expertise as a Lab Engineer with the esteemed Mechatronics Department, UET Peshawar, for two impactful years, from 2019 to 2021. His passion for exploring the potential of these cutting-edge technologies shines through in his research, where he strives to push the boundaries of knowledge and make a positive impact on society. With an insatiable thirst for innovation and a dedication to scientific inquiry, he is undoubtedly an emerging force in the field of research, poised to make significant contributions to the advancement of technology, and its applications in the medical domain.

GHASSAN HUSNAIN received the B.E. degree, the M.Sc. degree in network systems from the University of Sunderland, England, in 2011, and the Ph.D. degree in intelligent transportation systems (ITS) from the University of Engineering and Technology, Peshawar, Pakistan, in 2021. He is currently an Associate Professor with the Department of Computer Science, CECOS University of IT and Emerging Sciences, Peshawar. His research interests include intelligent systems, ad hoc networks, evolutionary computation, bio-inspired algorithms, soft computing, and artificial intelligence.

SYED ALI FARAZ JAFFERY received the B.S. degree in electronic engineering from the University of Engineering and Technology (UET), Taxila, Pakistan.

He worked as a Research Engineer at the Syndicate of Embedded and Electronic Design (SEED), UET Taxila, and the National Centre for Artificial Intelligence (NCAI), UET Peshawar, Pakistan. He is currently undergoing training in chip design and verification with Nomaniyat and 10x Engineer, Lahore, Pakistan.